

DESIGN OF EXPLOSION ISOLATION BARRIERS

P E Moore and D J Spring

Kidde plc., Mathisen Way, Poyle Road, Colnbrook, Slough, SL3 0HB, UK

INTRODUCTION

Industrial plants involve multiple interconnected pieces of equipment, such as spray driers, cyclones, bag filters, grinders etc. Explosion isolation is an important part of the design of any overall industrial process plant explosion protection system. Explosion isolation barriers include triggered suppressant barriers and triggered high-speed gate valves installed on the interconnecting ducts between process plant components. The design purpose of an explosion isolation barrier is to prevent, or at least to minimise, the possibility that an explosion starting in one piece of equipment propagates along the duct network to adjoining items of the plant¹⁻⁴. Clearly, it is essential that the barrier, either suppressant or gate valve, be established before the flame has passed the barrier location on the duct. The actual siting of the barrier along the duct depends critically on an understanding of the factors affecting the speed of flame propagation into and along ducts.

Early literature in this area concentrated on the study of the propagation of explosions of interest to the mining industry, e.g. coal dust and methane gas⁵⁻¹⁰. It is only in the last 10 years or so that a significant corpus of literature has been built up on the propagation of flames along ducts or interconnected process equipment such as conveyors or elevator legs where explosible fuels of industrial relevance are present. Lunn and co-workers at HSL undertook an extensive test programme that quantified the course of industrial explosions between interconnected vessels. This work culminated in definitive guidance on the pressure development in the primary and secondary (connected) vessels, although no results were reported on the flame propagation down the interconnected duct^{11,12}. Crowhurst also studied pressures developed as dust explosions propagate through ducts¹³. Degeest presented results on flame acceleration in elongated vessels and pipes¹⁴. Chatrathi and Going et al. have published results on gases¹⁵⁻¹⁷ and metal dust explosion propagation^{18,19} in pipes. One of the most recent and comprehensive studies of explosion propagation between interconnected vessels is that undertaken by the Forschungsgesellschaft für angewandte Systemsicherheit und Arbeitsmedizin (FSA) at their test site in Kappelrodeck^{20,21}. These researchers report results using several different vessel and duct sizes with both propane and maize starch fuels. However, apart from one general paper²² there is no detailed guidance established in the literature as to how this body of experimental data could be used as a basis for the design, especially the placement, of explosion isolation barriers.

BASIC PRINCIPLES

The design of explosion isolation systems requires a fundamental understanding of the time course of the pertinent events. These principles are described below. They have

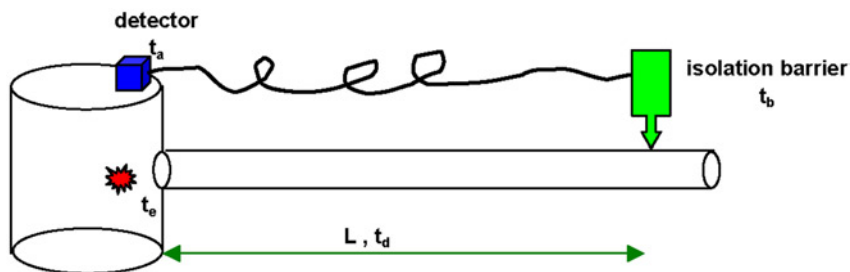


Figure 1. Schematic of an isolation system

been engrossed by the authors into a modelling tool, SmartISTM, for the design of explosion isolation barriers. Successful operation of the barrier, which can be either a fast-acting valve or a suppressant barrier, requires that the barrier be established to block progress of the flame before the flame arrives at the position of the barrier. Mathematically, we can express this as follows:

$$t_a + t_b < t_e + t_d \quad \text{ms} \quad (1)$$

where t_a is the time from ignition at which the explosion is detected, t_e the time (also from ignition) at which flame enters the duct, t_b the time taken for the given barrier to be established once the explosion has been detected by the detector, and t_d the time taken for the flame to travel the distance d down the duct to the position of the barrier (see Figure 1).

Clearly, t_b is a known parameter, since it depends only on the specific barrier hardware chosen and on the duct diameter. For fast-acting valves, t_b is the experimentally determined time taken for the valve to close and, in general, the larger the diameter of the duct, the longer this time will be. For suppressant barriers, t_b is the time taken for the discharged suppressant cloud to traverse the width of the duct and to establish an extinguishing concentration sufficient to prevent flame propagation. Again, this is an experimentally determined parameter and, in general, the larger the diameter of the duct, the longer this time will be. Other relevant factors that affect the suppressant barrier establishment time, t_b , are the orifice diameter of the suppressor, the propelling agent pressure, and the mode of mounting of the suppressor on the duct. Use of hoses or elbows results in increased t_b . Note that in applications where an interconnected vessel is designed for explosion containment or explosion venting, the suppressant barrier needs to be sustained for the duration of the explosion event.

The detection time, t_a , is dependent on the type of explosion detection device used. Pressure detectors (threshold or rate-of-rise) are usually mounted¹ on the protected vessel,

¹The installation of a pressure detector on, or in the vicinity of a duct, is not advised because the detector response will be adversely affected by the pressure losses down the interconnected duct, especially that at the mouth of the duct. This pressure loss will result in delayed detection of the explosion.

whereas flame detectors are typically mounted on the duct, close to the junction with the source vessel. For pressure detectors, the detection time t_a depends on the source vessel volume and shape, the intrinsic explosibility parameters of the fuel, the actual fuel concentration in the vessel and its distribution, and the initial conditions of temperature and pressure, oxygen concentration, and turbulence prevailing in the vessel. For optical flame detectors, detection takes place when the flame enters the duct and comes into the field of view of the flame sensor. This time, t_e , depends on the same set of parameters as for t_a but, in addition, is also dependent on the ignition location relative to the duct mouth and any process fluid flow. Both of these times can be calculated using standard models of explosion development^{23–27}.

The flame propagation time, t_d depends on the duct size, barrier location, the process fluid flow, and the flame velocities in the duct. Thus, a modelling tool to determine a safe location for an isolation barrier has to calculate the value of the distance d , such that Equation 1 is just satisfied. This value is then the minimum barrier distance, d_{min} .

Siwek and Moore²² defined the instantaneous velocity of the flame front, v_{ff} , as the sum of three component velocities:

$$v_{ff} = v_{air} + v_p + v_f \quad \text{m/s} \quad (2)$$

- v_{air} is the bulk air velocity existing prior to the start of the explosion. Note that this can be positive (flow away from the vessel) or negative (flow into the vessel) depending on the precise nature of the process under consideration. Obviously, the latter will hinder flame propagation away from the vessel. However, it is likely that, at some point, the developing explosion pressure in the vessel will overcome this process air flow. Thus, on conservative grounds, it is better to ascribe an inflow as $v_{air} = 0$, rather than as a negative value.
- v_p is the instantaneous pressure piling component of velocity due to the increasing pressure in the source vessel from the developing explosion.
- v_f is the instantaneous flame speed component i.e. the movement of the flame through the (moving) air and its acceleration due to turbulence and flame stretch in the duct.

CALCULATION OF v_p

The increase in pressure with time arising from the developing explosion in the source vessel can be modelled using standard mathematical treatments^{23–27} with input of appropriate parameters such as the vessel volume, V , the ambient temperature and pressure, and the fuel burning velocity. This latter parameter is generally derived from the measured fuel explosibility rate constant, K_{max} ². If the source vessel is vented, or protected by an explosion suppression system, the explosion development is assumed to occur up until the point at which the appropriate reduced (suppressed or vented) explosion pressure, P_{red} , is reached, after which point no further increase in pressure is assumed to take

² K_{max} is the measured maximum rate of pressure rise, normalised to a volume of $V = 1 \text{ m}^3$.

place. In reality, the pressure will start to fall after P_{red} is reached, but on conservative grounds this is ignored. If the source vessel is closed (contained explosion condition), then the explosion is assumed to continue until the maximum explosion pressure, P_{max} , is reached. Once the flame front reaches the duct entrance, the pressure piling component of velocity can be calculated by an equation of the form:

$$v_p = a \left(\frac{P}{\rho_a (1 + \frac{1}{2}P)} \right)^b \quad \text{m/s} \quad (3)$$

where P is the instantaneous pressure in the vessel in bar(g), ρ_a is the density of air under the prevailing process conditions in kg/m^3 , and the constants a and b are determined by best fit to the literature experimental data. Equation 3 can be derived either by a simplification of the standard fluid dynamic equations²⁸ for flow through a duct or from that of flow through an orifice. At low pressures these become equivalent.

CALCULATION OF v_f

It is assumed that the flame speed component, i.e. the movement of the flame front through the moving air will increase as the distance travelled down the duct increases. This is a known phenomenon, and arises because the induced turbulence increases fuel-air mixing and so enhances the burning rate^{3,14}. Degeest¹⁴, from a study of flame velocities in elongated vessels, argues that flame velocity increases in proportion to the square root of the length to diameter ratio. A modification of this is used to model v_f :

$$v_f = jS_f \{1 + (d/D)^k\} \quad \text{m/s} \quad (4)$$

where S_f is the flame velocity prevailing in the source vessel, d is the instantaneous distance travelled along the duct, D is the diameter³ of the duct, and j and k are constants determined by best fit to the experimental data and which depend on the nature of the fuel.

VALIDATION

The FSA data^{20,21} were used to determine the best values for the constants in Equations 3 and 4 and to validate the projections against experimental results in establishing a calculation tool. The FSA test work involved the use of 0.5, 1.0, 4.25 and 9.4 m^3 explosion vessels connected by ducts of various diameters in the range 100–400 mm, along which were mounted pressure and flame sensors, such that the times for the flames to pass given locations could be measured. In the case of two interconnected vessels, the explosion was initiated in the smaller vessel, which was either closed (apart from the

³For ducts of rectangular cross-section, the equivalent diameter is used.

interconnecting duct) or vented. In this way, a range of P_{red} values could be generated by changing the vent area. For some of the tests, a pneumatic conveying system was in operation. Explosions were generated in the vessels under ISO6814²⁹ conditions. Most of the tests were undertaken with maize starch fuel, which was dried to a moisture content of <4% and whose explosibility parameters⁴ were $K_{max} = 190$ bar.m/s and $P_{max} = 10$ bar(a). The other principal fuel used was quiescent propane with $K_{max} = 100$ bar.m/s and $P_{max} = 9$ bar(a). Both the maize and propane fuels were used at a range of concentrations.

The data in the FSA papers were presented graphically as the time the flame front takes to reach a given sensor station with the results of several experiments being given for each configuration. In all cases, for the purposes of this model, the shortest of these experimental times for each station was taken for the base data set. Thus, the model is optimised to the worst case FSA results. In order to determine the best fit to the modelling constants in Equations 3 and 4, it was assumed that the flame velocity varied linearly with distance along the duct, and that the pressure in the source vessel was at P_{red} . In this way, the time t_{ff} taken for the flame to reach a given sensor at distance L along the duct is then given by $t_{ff} = L / (v_{air} + v_p + v_f)_{average}$ with v_p and v_f calculated by Equations 3 and 4 respectively. The numerical constants were then adjusted to give the best fit between the experimental and calculated times which, in terms of Equation 1, are $t_e + t_d$, since they are measured from ignition. Figures 2 and 3 show the experimental and calculated times for the flames to reach different positions down the duct for dust and propane explosions respectively.

Having set the parameters for Equations 3 and 4, a computer model was constructed to start at ignition in the source vessel and to step through increments of time calculating the pressure and size of the explosion in the source vessel, taking into account the input P_{red} , as described above. At the appropriate point, the flame enters the duct, and Equations 3 and 4 are used to calculate the flame velocity and position for each time step. The results were checked against another set of experimental data available to us, which derived from tests undertaken in 1993 at the Swiss Safety Institute in Zeglingen and commissioned by Kidde Plc to underpin the design parameters involved with suppressant barriers. Tests were carried out using a 2.4 m³ vessel connected to a 400 mm diameter duct. Dust explosions of various severities ($K_{max} = 123, 183$ and 300 bar.ms⁻¹ and $P_{max} \sim 9$ bar(g)) were ignited in the vessel, which was also fitted with a variable explosion vent disc such that different P_{red} values could be generated. Optical flame sensors were located at up to 4 positions along the duct. The first 21 tests were undertaken to measure flame speeds, explosion pressures and flame front position along the duct with respect to time. Figure 4 shows the experimental and calculated times for the flames to reach different positions down the duct. Again, in terms of Equation 1, these times are $t_e + t_d$, since they are measured from ignition.

In this way, it is possible to calculate the minimum effective distance at which the barrier can be located from the mouth of the duct. Figure 5 shows the modelled and

⁴As determined in accordance with ISO6814.

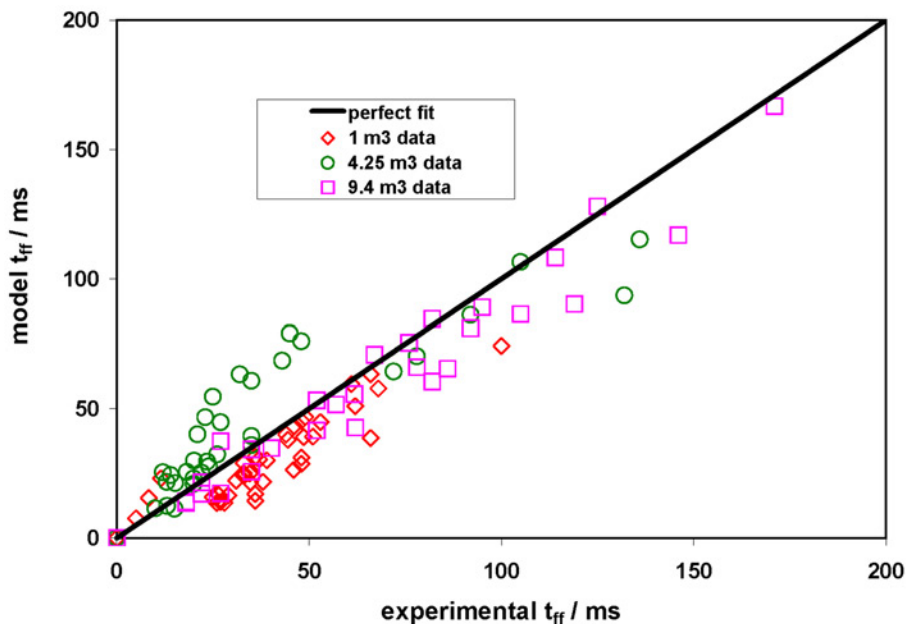


Figure 2. Comparison of experimental and modelled times: FSA dust explosion data

experimental distance – time plots for a test with $K_{\max} = 123$ bar.m/s and a $P_{\text{red}} = 0.88$ bar(g), and Figure 6 those for a test with a $K_{\max} = 300$ bar.m/s and $P_{\text{red}} = 1.12$ bar(g). Note that time is measured from ignition.

SENSITIVITY ANALYSIS

In the foregoing sections, the core mathematical model of explosion development and of flame propagation along a duct has been described, along with its underpinning by data from major experimental test work by third parties. We now need to consider how to use this model to calculate barrier locations for explosion situations that are likely to arise.

IGNITION LOCATION

Pressure detectors have to be mounted onto the source vessel, and the same detector can also trigger any suppression system, if fitted. We can understand the factors affecting barrier performance by considering Equation 1. For pressure detection, t_a is fixed only by the detection system; typically this will be set at 50 mbar, and t_a will be approximately proportional to $V^{1/3}/K_{\max}$. Thus, the more severe explosions, or those in smaller vessels,

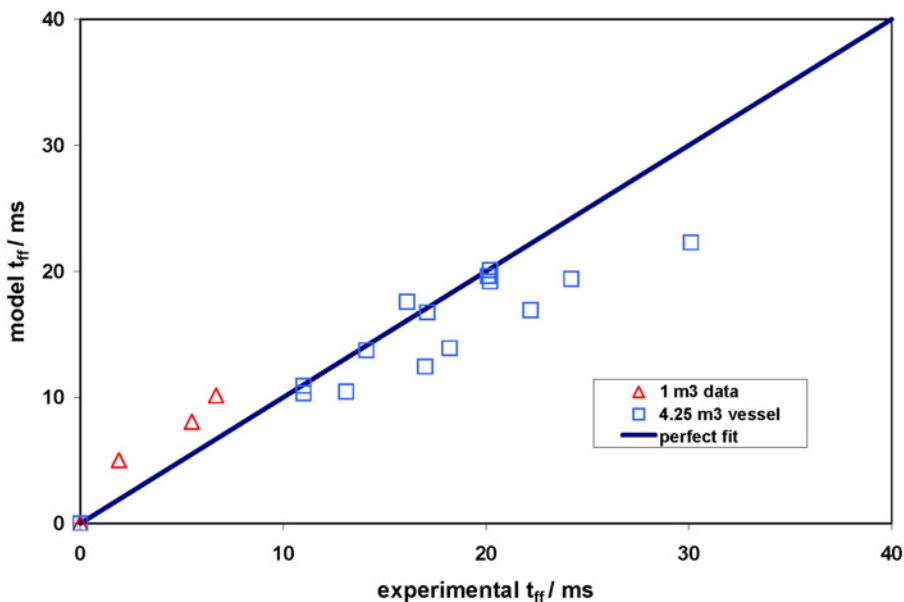


Figure 3. Comparison of experimental and modelled times: FSA propane explosion data

will be detected sooner. Likewise, the time to close the barrier, t_b , is fixed, and only depends on the selected hardware and the duct diameter. Obviously, the worst case for a barrier system is when the right hand side of Equation 1, $t_e + t_d$, is as small as possible. A major input to the time to duct entry, t_e , is the distance of the ignition location relative to the mouth of the duct, so clearly a worst case scenario will be where this distance is minimised. This runs counter to the perceived wisdom of experimentalists' work with closed vessel explosions, where the worst case explosions are judged⁵ to arise with ignition located essentially in the centre of the vessel. We can illustrate this with a typical system, e.g. for a 50 m³ vessel attached to 400 mm diameter duct, with a dust explosion of $K_{max} = 200$ bar.m/s. Using a 50 mbar detection pressure, the model predicts that the explosion will be detected approximately 90 ms after ignition and, unless the ignition occurs within about one half of the vessel radius from the duct mouth, the explosion will always be detected before the flame front has entered the duct. Whether a barrier will ultimately be successfully established will depend on the relative magnitudes of t_b and t_d . This is further demonstrated in Figure 7 for the same scenario, where the calculated

⁵Ignition in the geometric centre of the vessel normally gives rise to the highest explosion parameters because wall quenching of the propagating flame front is minimised.

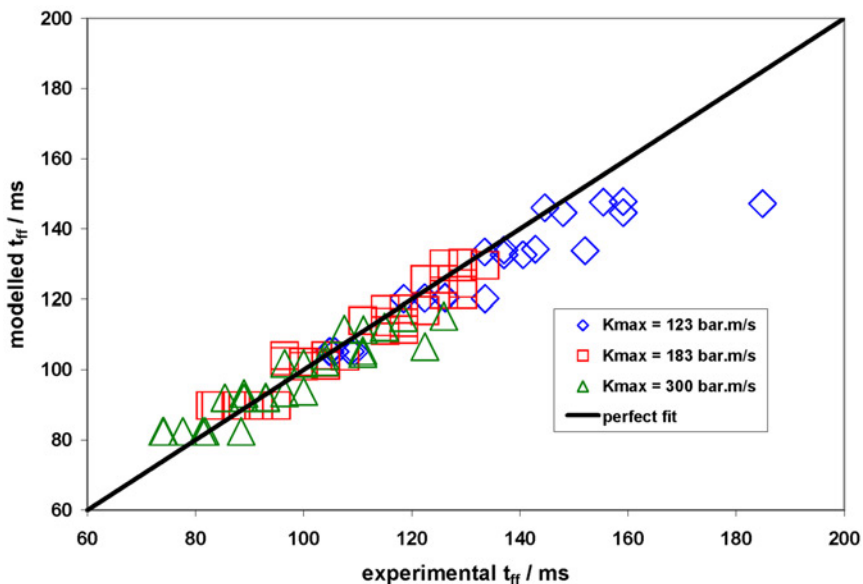


Figure 4. Comparison of experimental and modelled times: 2.4 m³ dust explosion data

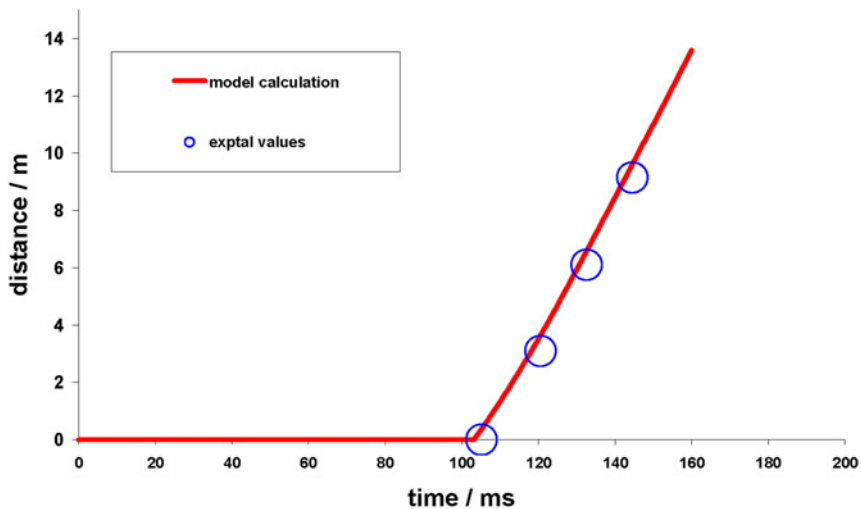


Figure 5. Modelling of Zeglingen data: flame position with time

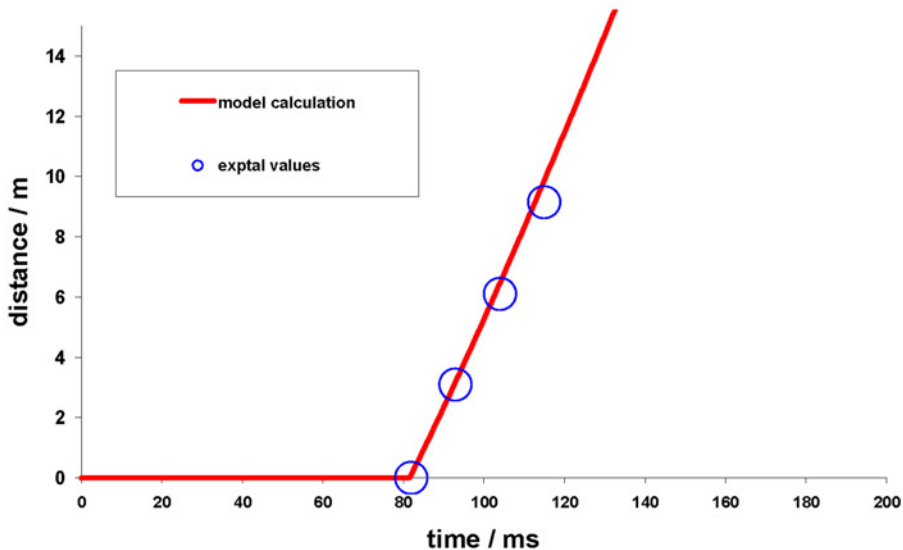


Figure 6. Modelling of Zeglingen data: flame position with time

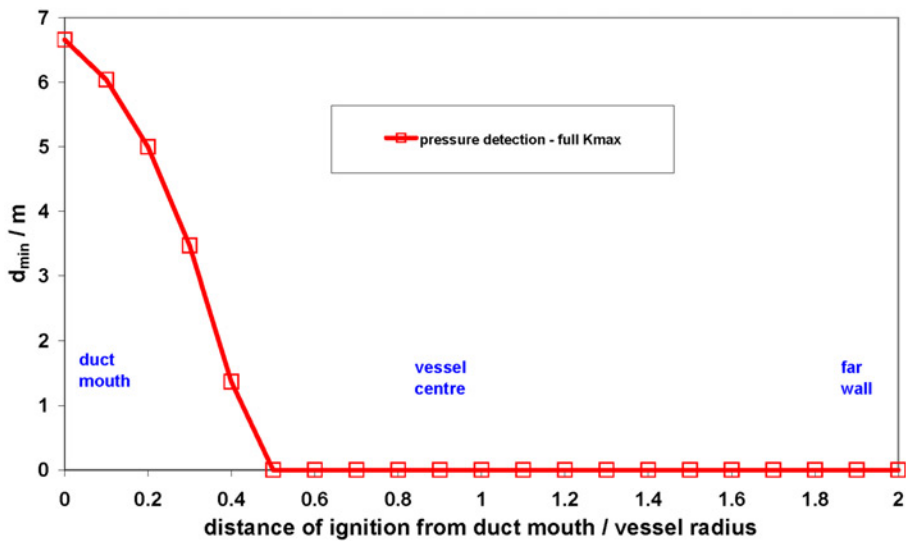


Figure 7. Effect of ignition distance from duct mouth on minimum barrier distances

minimum barrier distances from the duct mouth are plotted as a function of ignition location. Inspection of the figure shows that, for this configuration, locating the barrier close to the duct mouth is sufficient provided that ignition occurs towards the centre of the vessel. Note that, once the flame front reaches the vessel wall, quenching will reduce the rate of increase of pressure and the rate of growth of fireball radius. Conservatively, this wall effect has been ignored.

This analysis clearly demonstrates that with pressure as the means of detection, central ignition as per ISO 6814/4²⁹, is far from being a worst case scenario. Moreover, this indicates that many of the experimental studies of isolation systems, as well as any design guidance arising from them, are fundamentally flawed through the use of central ignition as representing the worst case scenario. The consequence is that there may be a larger residual risk in reliance on the efficacy of such systems than was once realised.

As a result of this and similar analyses of many other configurations of vessel, explosion severity and duct diameter, for the SmartIS software ignition has been assumed to take place at an *a priori* dimension of 0.3 times the equivalent radius of the vessel from the duct mouth. The consequence in this particular example is a barrier minimum distance, d_{\min} , of around 3.5 m, which is taken to be a representative of a near worst case scenario. Obviously, all other factors being equal, if the ignition were closer, requiring a longer d_{\min} , there is an attendant risk that the barrier would then fail to mitigate explosion propagation. It follows from this assumption that there is a residual risk implicit in the design of such explosion isolation barriers. To quantify this exposure we need to consider the relative volumes of a sphere of radius a , and a hemisphere of radius $0.3a$. It can be shown that the hemisphere represents less than 1.4% of the volume of the sphere. Expressed otherwise, a d_{\min} of around 3.5 m will protect against ignitions occurring in 98.6% of the vessel volume, assuming:

- (i) that all locations in the vessel are equally likely as sites for ignition, and
- (ii) that all those ignitions are limit cases in terms of explosion severity and flame propagation, and lead to worst case situations regarding d_{\min} .

Note that this certainly does not mean that the barrier would be ineffective in 1.4% of cases; because of the very low probabilities of either of these provisions being met. The reliability and the effective residual risk of barrier design is considered in more detail below.

For optical flame detection, other considerations apply. Since the flame will be detected essentially at the instant it enters the duct (there is a general requirement to install the detector within a couple of diameters from the duct mouth), ignition near the duct mouth is the easy scenario. This also means that $t_a = t_e$. The worst case is now ignition remote from the duct mouth, as shown in Figure 8 for the same scenario as for Figure 7. The reason for this is that there is then a longer time available for the explosion pressure to develop and, consequently, the pressure piling component of velocity, v_p , at the moment of entry of the flame into the duct is higher, thus t_d in Equation 1 is shorter.

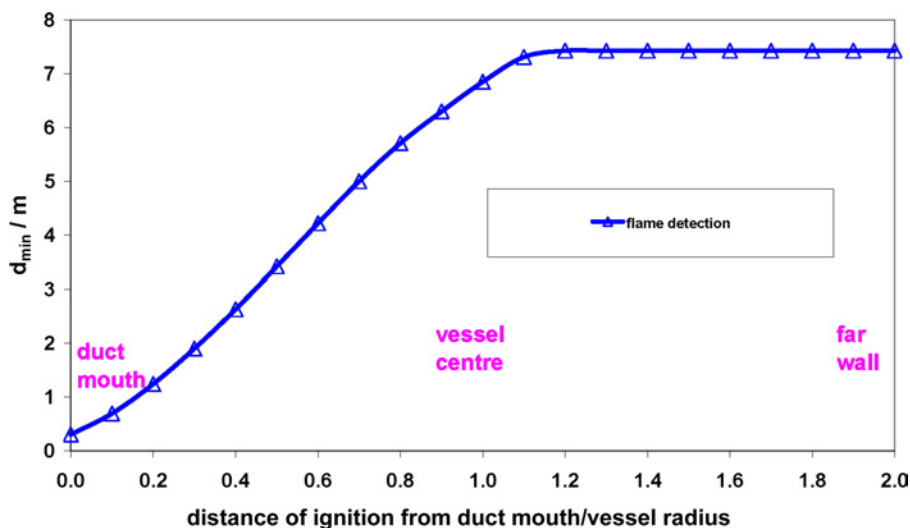


Figure 8. Effect of ignition distance from duct mouth on minimum barrier distances

Inspection of Figure 8 indicates that the calculated d_{\min} increases as the ignition location is moved to the centre of the vessel but, beyond about $1.1 \times$ radius, there is no further increase. The reason for this is that there is an effective limit on v_p , which can not exceed the speed of sound in air (ignoring the fact that the speed of sound in dust-laden air may be less than that in free air). SmartIS takes the worst case scenario as ignition on the far wall of the vessel from the duct mouth when the detection means is a flame detector.

This importance of ignition location in determining the outcome of a barrier isolation scenario has been further demonstrated by the authors by calculations with an industry standard CFD explosion modelling tool — FLACSTM.³⁰ A scenario was set up using a 2.4 m³ vessel (1.2 m diameter, 2 m length) connected co-axially to a 14 m long by 400 mm circular duct. The vessel and duct were filled with quiescent stoichiometric propane-air. Point ignition was located on the axis of the vessel at five different positions of 0.25, 0.65, 1.05, 1.45 and 2.05 m from the mouth of the duct and is indicated by the white square in Figure 9. The figure shows the position of the flame fronts for the five scenarios at 180 ms after ignition and clearly demonstrates that the closer the location of ignition to the duct mouth, the sooner the flame reaches a given position in the duct.

EXPLOSION SEVERITY

Assuming worst case ignition locations as outlined above, for both optical flame detection and pressure detection ($P_a = 50$ mbar), calculations were undertaken for dust explosions

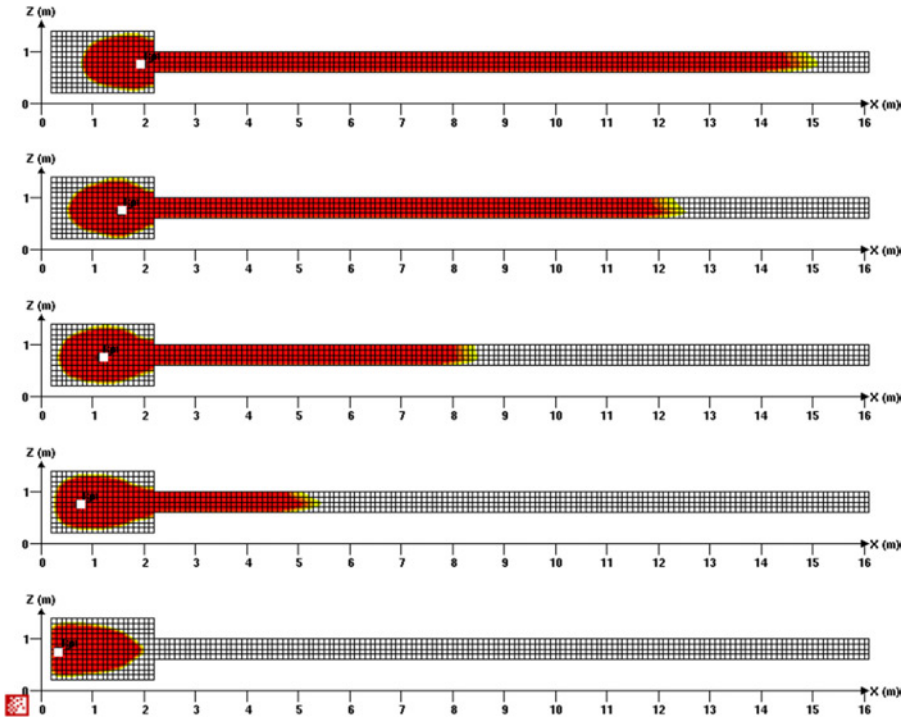


Figure 9. Flame front position at 180 ms for various ignition locations calculated with FLACS™: 2.4 m³ vessel + 14 m × 400 mm duct: quiescent stoichiometric propane air

over a range of K_{max} and vessel volumes. The minimum distances so calculated are shown in Figure 10 plotted against the parameter $K_{max}/V^{1/3}$.

Inspection shows that, for pressure detection, there is a strong dependence on K_{max} , the weaker the explosion, the greater the d_{min} ⁶. Again, this indicates that the ISO conditions in terms of explosion severity are not always the worst case for barrier deployment. The reason for this is, of course, that the weaker explosion takes longer to reach P_a , so t_a is longer. Taking this into account, in the SmartIS model, the d_{min} calculation is performed twice, once with an explosion rate constant of K_{max} , and the second time using an *a priori* value of $K_{max}/3$. The program then conservatively defaults to the longer of the two distances. Although selection of $K_{max}/3$ appears to be arbitrary at first sight, in fact, it is based on standard measurements of dust explosibility as a function of concentration and stoichiometry. For most fuels, the concentration giving rise to an explosibility of

⁶Also, the bigger the vessel, the longer d_{min} .

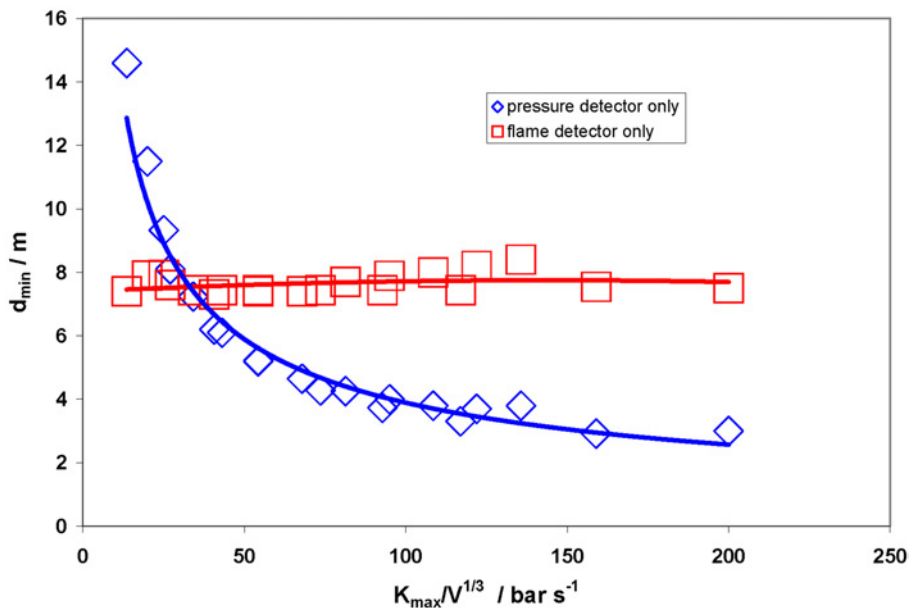


Figure 10. Minimum distance calculation as a function of $K_{\max}/V^{1/3}$

$K_{\max}/3$ is typically close to the minimum explosible concentration^{1–3,23}. Thus, assuming that all explosible concentrations are equally probable, the vast majority (>95%) of possible real explosions are covered by having SmartIS calculate for these two explosion rate constant values. Such an assumption remains valid provided that the process conditions of turbulence and homogeneity are sensible, relative to the test methodology that ascribed the fuel explosibility, K_{\max} . This assumption is considered further in the assessment of implicit residual risk discussed below.

MAXIMUM DISTANCES AND DETONATION LIMITS

There are limits on the maximum distance d_{\max} ⁷, that a barrier can be located from the source vessel which are defined by the criterion at which the deflagration wave is likely to transition into a detonation wave. In this context, there are known relationships between duct diameter and the transition from a deflagration to a detonation. For gases, based on the work of Bartknecht³ and Steen³¹, a conservative limit, d_{det} , of 40 diameters is taken as the maximum safe length of duct, up to a maximum of 15 m. A more recent review of the literature on the deflagration to detonation transition is given by Chatrathi

⁷SmartIS output arbitrarily defaults to $d_{\max} = d_{\min} + 5(\text{m})$ when $d_{\min} + 5 < d_{\text{det}}$.

and Going¹⁵. For dusts, a value of 80 diameters is assumed, up to a maximum of 20 m. If $d_{\min} > d_{\det}$, then SmartIS will not make any minimum distance prediction, since there is then no safe configuration of the barrier for the input conditions.

EXAMPLES OF SmartIS OUTPUT

Figure 11 shows the SmartIS output for a dust explosion in a 10 m³ vessel, protected by suppression or venting to give a P_{red} of 0.5 bar(g), with both a pressure detector mounted on the vessel and a flame detector located at the mouth of the 400 mm diameter duct. The isolation is provided by a powder suppressant barrier, delivered by a proprietary explosion suppressor. Because a suppressant barrier is used, there is now the requirement for an additional length of duct, in this case a minimum of 2.3 m is ascribed, before the next item of plant. This is to allow time for the suppressant to interact with the flame (the kinetics of suppression are finite; they do not occur in zero time). The flame and pressure detectors combine synergistically to result in a shorter minimum distance than if either alone had been used. When a pressure detector alone is used, the calculated corresponding minimum barrier distance is 3.2 m, and when a flame detector is used on its own the distance is 2.9 m.

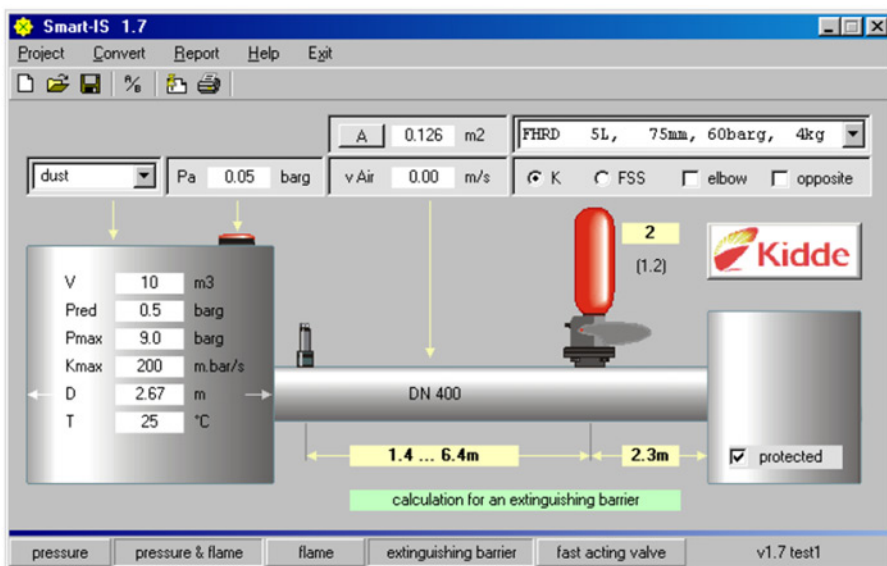


Figure 11. SmartIS prediction: dust explosion with a suppression barrier and both pressure and optical flame detectors

VALIDATION TESTS AT FSA: ATEX APPROVAL

During the period December 2002–June 2003, validation tests were undertaken of SmartIS designs by FSA at Kappelrodeck, Germany, as part of the ATEX approvals of Kidde explosion protection systems and hardware³². A summary of the tests with fast-acting valves is given in Table 1 and that of the suppressant barrier tests in Table 2. These were done with a 150, 300, 600 and 1000 mm diameter ducts connected to closed 1, 4.4, 9.7, or 26.5 m³ vessels. For suppressant barriers, a range of hardware was used. For all tests, pressure detection was used with a detection pressure of 50 mbar. The following explosion threats were used:

dust 100	maize starch	$K_{\max} = 100 \text{ bar.m/s}$	$P_{\max} = 10 \text{ bar(a)}$
dust 300	maize starch	$K_{\max} = 300 \text{ bar.m/s}$	$P_{\max} = 10 \text{ bar(a)}$
quiescent gas	propane	$K_{\max} = 100 \text{ bar.m/s}$	$P_{\max} = 8.8 \text{ bar(a)}$
turbulent gas	propane	$K_{\max} = 500 \text{ bar.m/s}$	$P_{\max} = 9.8 \text{ bar(a)}$
hybrid	maize starch & propane	$K_{\max} = 400 \text{ bar.m/s}$	$P_{\max} = 11 \text{ bar(a)}$

Because SmartIS reports minimum and maximum distances (see above) for siting the valve from the source vessel, many of the tests were done at both the minimum and maximum distances. For some of the gas and hybrid cases, the SmartIS model would not predict a minimum distance, because the distances needed were longer than its conservative limits for transition to detonation. In these cases the barrier locations were estimated by hand on the basis of the mathematical model. Ignition location was at the discretion of the certifying body – at the centre of the vessel, or at locations close to or remote from the duct entry.

Table 1. Fast acting valve tests

Vessel Volume m ³	Explosion	Duct mm	SmartIS Distances m	Test Distances m	Result
1	dust 300	150	5.4–10.4	5 & 11	Tests successful
1	quiescent gas	150	detonation limited	5 & 8	Tests successful
1	hybrid	150	detonation limited	8	Test successful
4.4	dust 300	150	4.0–9.0	5 & 10	Tests successful
4.4	dust 300	150	4.7–9.7	5 & 10	Tests successful
4.4	dust 300	300	7.7–12.7	7.7 & 12.7	Tests successful
4.4	turbulent gas	300	detonation limited	5.0 & 8.0	Tests successful, but pressure at valve > 15 bar (8 m location)
4.4	turbulent gas	150	detonation limited	5.0	Test successful

Table 2. Suppressant barrier tests

Vessel Volume m ³	Explosion	Duct mm	SmartIS Distances m	Test Distances m	Result
4.4	dust 300	200	8.6–13.6	8.6 & 13.6	Tests successful
4.4	dust 300	300	3.3–8.3	3.3	Test successful
4.4	dust 100	300	4.2–9.2	4.2	Test successful
4.4	dust 300	300	2.5–7.5	2.5 & 7.5	Tests successful
4.4	quiescent gas	300	8.9–12	8.9 & 12	Tests successful
4.4	turbulent gas	300	detonation limited	3.7 & 8.7	Tests successful
4.4	dust 100	300	4.2–9.2	4.2	Test successful
4.4	dust 300	300	2.5–7.5	2.5	Test successful
4.4	quiescent gas	300	8.9–12	8.9	Test successful
4.4	turbulent gas	300	detonation limited	3.7	Test successful
9.7	dust 300	600	3.4–8.4	3.4	Test successful
26.5	dust 300	1000	4.3–9.3	4.3	Test successful

As can be seen from an inspection of Tables 1 and 2, in all cases, the barrier was successfully established before the flame front arrived, and no flame breakthrough was observed. Although this observation also applies to the gas and hybrid explosions for which SmartIS was unable to produce a distance prediction, it was evident that the mode of flame propagation in the duct was close to, or had entered, the deflagration to detonation transition zone in these tests.

It should also be noted in considering Table 2 that most of the tests involved closed vessels. In a couple of the tests, flame sensors mounted downstream of the barrier detected flame at long times (several hundred ms) after ignition, and long after the suppressant barrier had been deployed and the explosion isolated. This is probably a consequence of all of the suppressant having been swept out of the duct, leaving the way clear for some further transport of flame and hot gases from the closed source vessel. Such a scenario is not an issue when the interconnected vessels are fitted with an explosion suppression system. For contained and vented explosions this can be overcome by providing a sustained discharge of suppressant at the barrier location.

RESIDUAL RISK

In ascribing the efficacy of any explosion protection measure, it is important to consider the limitations of effectiveness, and thus the prevailing residual risk in adopting the protection means. For the design of explosion isolation means these considerations are particularly prevalent.

The mission of an explosion isolation barrier system is to prevent flame propagation that arises from an explosion initiated in one part of the process from propagating to an

adjacent part of the process. It is particularly important to de-couple processes such as milling where there is a higher risk of ignition from processes such as storage silos where the volumes and fuel loads mean that there is a higher consequence from an explosion. It is also intuitively clear that any ignition that is in close proximity to the barrier location cannot be mitigated by the protection measure.

Put simply, no barrier system is a 100% foolproof system. If the process safety of an industrial plant is critically dependent on the effectiveness of an explosion barrier isolation means, such as would be the case if flame propagation beyond a barrier location would result in a subsequent explosion in an unprotected plant component, then such a process has an implicit residual risk of explosion consequences. To define explosion isolation barrier efficacy we need to consider the implicit assumptions in the design tool. According to the European Directive 94/9/EC³³ suppliers of protection systems have to provide an estimate of the residual risk of the system not fulfilling its protection mission. The principles that underpin the SmartIS design tool assume that the ignition occurs in the vessel, and not beyond the mouth of the interconnected duct, and that the ascribed explosibility parameters are a meaningful representation of the prevailing explosion hazard. Clearly, if the risk of an ignition in the duct is adjudged as unacceptable, then this explosion protection mitigation means is, *de facto*, an insufficient or inappropriate measure.

For isolation barrier systems that use a combination of flame and pressure detection, a solution for barrier distance can be derived for all ignition location scenarios within the vessel, and system reliability is subject only to the pertinence of the ascribed explosibility, the barrier design, and the reliability of the installed hardware. For systems that elect only to use pressure detection, the implicit assumptions on ignition location and K_{max} used to define d_{min} imply a definable additional residual risk. Figure 12 sets out this residual risk for the two different scenarios, calculated as a function of the actual explosion intensity K , relative to K_{max} . Here we see that for the large vessel volume, high K scenario (red squares in the figure), the longest minimum distance is determined by the K_{max} explosion, and the residual risk exceeds the SmartIS datum for conditions of $K > K_{max}$ and $K \ll K_{max}/3$. For the small vessel volume, low K scenario (blue circles in the figure), the longest minimum distance is determined by the $K_{max}/3$ explosion, and the SmartIS datum is only exceeded for conditions of $K < K_{max}/3$.

Put another way, in the practice of selecting the SmartIS design criteria when detection is by pressure detection only, there is a residual risk that maybe one explosion in 200⁸ will result in some flame propagation beyond the barrier location. The authors consider that the implicit assumptions embedded within the model represent an appropriate compromise between practicality and residual risk. However, for each application, the pertinence of the residual risk must be considered as part of the process safety study.

Users of explosion isolation barriers as the primary explosion protection means would be advised to avoid systems that rely only on pressure detection in applications where the downstream consequence of flame propagation is considered significant.

⁸Indicative estimate based upon the portfolio of expected explosion scenarios.

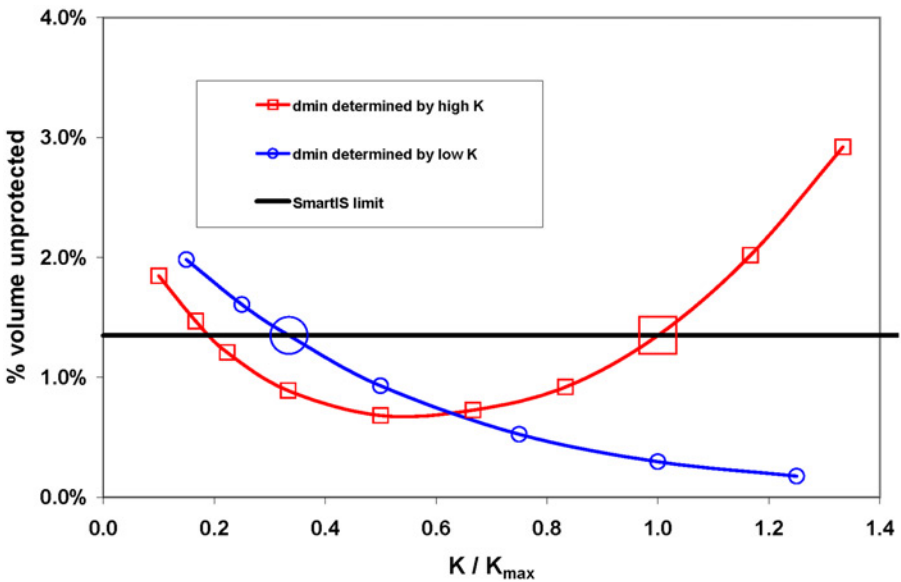


Figure 12. Sensitivity of risk to explosion severity for pressure detection only

Users of the SmartIS design tool that elect to locate barriers closer than the ascribed minimum distances implicitly accept a higher residual risk.

CONCLUSIONS

1. This paper has shown that, from an understanding of the basic science involved, and from the premise that the flame velocity can be broken down into three components, those of:
 - pre-existing process air velocity,
 - pressure piling velocity due to the developing explosion,
 - flame acceleration through turbulence and flame stretch,
 it has been possible to derive algorithms governing the propagation of gas and dust explosion flames along ducts that accord with experimental results. The algorithms have been validated using two independent, third party, sets of experimental data. These algorithms can be used to determine the positioning of the isolation barriers, either fast-acting valves or suppressant barriers, along the duct. The SmartIS software that incorporates these algorithms is an integral part of the System's ATEX certification.
2. Considerable understanding has been gained of the factors affecting the performance of barrier systems, particularly the true worst case scenarios. It has been found that

there is a dependence on the means of detection used:

- For pressure detection, the worst case is ignition close to the mouth of the duct and/or weak/soft explosions in large volumes.
 - For flame detection, the worst case is ignition remote from the mouth of the duct and strong (full K_{max}) explosions.
 - Use of dual sensor detection optimises the strengths of pressure detectors and flame detectors, and avoids their respective weaknesses in these scenarios.
3. The perceived wisdom of deployed barrier system design may have been less efficacious, because it depended on interpolation from tests that selected intense centrally ignited explosion scenarios.
 4. The implicit residual risk (limitation of efficacy) of an explosion isolation barrier designed using these algorithms can be ascribed by reference to the implicit assumptions within the model.

REFERENCES

1. Steen, H., 2000, *Handbuch des Explosionsschutzes*. New York: Wiley-VCH.
2. Eckhoff, R. K., 1991, *Dust Explosions in the Process Industries*. 1st ed: Butterworth-Heinemann Ltd.
3. Bartknecht, W., 1981, *Explosionen.*: Springer.
4. Bartknecht, W., 1987, *Staubexplosionen.*: Springer Verlag.
5. Bartknecht, W., 1971, Brenngas- und Staubexplosionen, Bundesinstitut für Arbeitsschutz, **F45**.
6. Bartknecht, W., 1974, *Course of Dust Explosions and their Control*, in *Loss Prevention Symposium*, pp. 159.
7. Bartknecht, W. and Scholl, E. W., 1967, *Automatische Löschung von Grubenexplosionen in Rohren mit Grossen Querschnitten*, in *12th International Conference of the Bergbau Versuchsstrecke*, Dortmund, pp. Paper R004.
8. Lieberman, J., Richmond, J. K. and Grumer, J., 1975, *Triggered Barrier Systems for the Suppression of Coal Dust Explosions*, in *16th International Conference on Coal Mine Safety Research*, pp. 4.1–4.18.
9. Lieberman, J., Richmond, J. K., Pro, R., Conti, R. and Cary, J., 1979, Triggered Barrier Systems for the Suppression of Coal Dust Explosions, US Bureau of Mines, **RI 8389**.
10. Pineau, J. P. and Ronchail, G., 1987, Propagation of Dust Explosions in Pipes, *ASTM Special Technical Publication*, **958**: 74–89.
11. Lunn, G. A., Holbrow, P., Andrews, S. and Gummer, J., 1996, Dust Explosions in Totally Enclosed Interconnected Vessel Systems, *J Loss Prevention Process Industries*, **9**(1): 45–58.
12. Holbrow, P., Andrews, S. and Lunn, G. A., 1996, Dust Explosions in Interconnected Vented Vessels, *J Loss Prevention Process Industries*, **9**(1): 91–103.
13. Crowhurst, D., 1989, Small Scale Dust Explosions Venting Through Ducts, *Archivum Combustionis*, **9**(1/4): 361–378.
14. Degeest, G. J., 1992, Course of Dust Explosions in Elongated Vessels, *Europex Newsletter*, (September): 4–6.

15. Chatrathi, K. and Going, J., 1996, Pipe and Duct Deflagrations Associated with Incinerators, *Process Safety Progress*, **15**(4): 74–89.
16. Chatrathi, K., 2000, Deflagration Protection of Pipes, *Hydrocarbon Engineering*, **5**(12): 72–76.
17. Chatrathi, K. and Going, J., 2001, Flame Propagation in Industrial Scale Piping, *Process Safety Progress*, **20**(4): 286–294.
18. Going, J. and Snoeys, J., 2002, Explosion Protection with Metal Dust Fuels, *Process Safety Progress*, **21**(4): 305–312.
19. Krone, V. and Going, J. E., 2001, Neue Erkenntnisse bei der Entkopplung von Aluminium-Staubexplosionen, *Technische Überwachung*, **Bd 42**(7–8): 17–22.
20. Roser, M., 1999, Investigation of Dust Explosion Phenomenon in Interconnected Process Vessels, Forschungsgesellschaft für angewandte Systemsicherheit und Arbeitsmedizin, Ph.D Thesis for University of Loughborough 1998,
21. Roser, M., Vogel, A., Radandt, S., Malalasekera, W. and Parkin, R., 1999, Investigations of Flame Front Propagation between Interconnected Process Vessels, *J Loss Prevention Process Industries*, **12**: 421–436.
22. Siwek, R. and Moore, P. E., 1997, Design Practice for Extinguishing Barrier Systems, *Process Safety Progress*, **16**: 244–250.
23. Nagy, J. and Verakis, H. C., 1983, *Development and Control of Dust Explosions*, ed. Kling, A. L. New York and Basel: Marcel Dekker Inc.
24. Nagy, J., Seiler, E. C., Conn, J. W. and Verakis, H. C., 1971, Explosion Development in Closed Vessels, United States Department of the Interior — Bureau of Mines Report of Investigations, **RI 7507**.
25. Bradley, D. and Mitcheson, A., 1976, Mathematical Solutions for Explosions in Spherical Vessels, *Combustion and Flame*, **26**: 201–217.
26. Nomura, S. I. and Tanaka, 1980, Prediction of Maximum Rate of Pressure Rise due to Dust Explosion in Closed Spherical and Non-spherical Vessels, *Ind. Eng. Chem. Process Des. Dev.*, **19**: 451–459.
27. Ogle, R. A., Beddow, J. K. and Chen, L. D., 1984, *Numerical Modelling of Dust Explosions*, in *Powder and Bulk Solids Handling and Processing, Technical Progress*, pp.
28. Perry, R. H. and Green, D. W., 1984, *Perry's Chemical Engineers' Handbook*. 6th ed. McGraw-Hill. Chapter 6.
29. ISO6814, 1985, International Standard: Explosion Protection Systems — Part 4: Determination of Efficacy of Explosion Suppression Systems, **ISO 6814/4**.
30. Gexcon, 2003, FLACS: (FLame ACceleration Simulator), Gexcon AS, Bergen, Norway,
31. Steen, H. and Schample, K., 1983, *Experimental Investigations of the Run-up Distances of Gaseous Detonation in Large Pipes*, in *4th International Symposium on Loss Prevention and Safety Promotion in the Process Industries*, pp. E23–E33.
32. Wingerden, K. v., 2004, Erfahrungen bei der ATEX-Zertifizierung von Explosionsschutzprodukten, *Technische Überwachung*, **45**: 18–21.
33. *European Directive on Equipment and Systems for Use in Potentially Explosive Atmospheres*, in *94/9/EC* 1994.